Environmental Science Nano

Accumulation of phenanthrene and its metabolites in lettuce (*Lactuca sativa* L.) as affected by magnetic carbon nanotubes and dissolved humic acids

Journal:	*Environmental Science: Nano*
Manuscript ID	EN-ART-09-2020-000932.R1
Article Type:	Paper

Environmental Significance

Phenanthrene (Phe) and its metabolites can accumulate in many terrestrial plants and cause carcinogenic and mutagenic toxicity to organisms via food chains. However, a recyclable and effective technique for poly aromatic hydrocarbon remediation has not been developed yet. Dissolved humic acids in soil are among the most active components. The present study investigated the behavior of Phe in *Lactuca sativa* L. as affected by magnetic carbon nanotubes (MCNTs) and DHAs in a hydroponic system. Our results demonstrated that MCNTs altered the Phe accumulation in lettuce seedlings and its combination with DHAs further alleviated the Phe- and metabolites-induced phytotoxicity. In addition, MCNTs could be easily separated from complex matrices that makes it a novel strategy for soil remediation using nano-enabled technology.

Accumulation of phenanthrene and its metabolites in lettuce (*Lactuca sativa* L.) as affected by magnetic carbon nanotubes and dissolved humic acids

Weili Jia[a, e, f], Chuanxin Ma[b, c, d, *], Mengfei Yin[a], Hongwen Sun[a], Qing Zhao[g], Jason C. White[c], Cuiping Wang[a, *], and Baoshan Xing[d]

[a]Key Laboratory of Pollution Processes and Environmental Criteria, Ministry of Education, Tianjin Key Laboratory of Environmental Remediation and Pollution Control, College of Environmental Science and Engineering, Nankai University, Tianjin 300071, China

[b]Key Laboratory for City Cluster Environmental Safety and Green Development of the Ministry of Education, Institute of Environmental and Ecological Engineering, Guangdong University of Technology, Guangzhou 510006, China

[c]The Connecticut Agricultural Experiment Station, New Haven, Connecticut 06504, United States

[d]Stockbridge School of Agriculture, University of Massachusetts, Amherst, Massachusetts 01003, United States

[e]SCNU Environmental Research Institute, Guangdong Provincial Key Laboratory of Chemical Pollution and Environmental Safety & MOE Key Laboratory of Theoretical Chemistry of Environment, South China Normal University, Guangzhou 510006, China

[f]School of Environment, South China Normal University, University Town, Guangzhou 510006, China

[g]Key Laboratory of Pollution Ecology and Environmental Engineering Institute of Applied Ecology; Institute of Applied Ecology, Chinese Academy of Sciences, Shenyang 110016, China

[*]**Corresponding authors:**

C.W.: E-mail: wangcp@nankai.edu.cn;

C.M.: E-mail: chuanxin.ma@gdut.edu.cn

Abstract

This study investigated the behavior of phenanthrene (Phe) in lettuce (*Lactuca sativa* L.) as affected by carbon nanotubes (CNTs)/magnetic carbon nanotubes (MCNTs) and dissolved humic acids (DHAs) under hydroponic conditions for 10 days. MCNTs alone or combined with DHAs reduced Phe accumulation in roots by more than 50%; in shoots, CNTs increased the Phe accumulation from 72.1 to 114.8%, regardless of the presence of DHAs. DHAs decreased the total Phe metabolites content in lettuce by 21.7-98.9%. Nine Phe-related metabolites were identified and a possible Phe metabolism pathway in lettuce was proposed. A positive correlation was found between Fe and Phe content in lettuce under treatments of MCNTs/CNTs combined with DHA1, indicating exogenous Fe in conjunction with DHA1 affected Phe accumulation in lettuce. Additionally, MCNTs/CNTs and DHAs reduced Phe-induced toxicity to lettuce by elevating the activity of shoot glutathione S-transferase (GST). The addition of MCNTs/CNTs alone and combination with DHAs enhanced photosynthesis. The upregulation of genes related to photosynthesis and carotenoid biosynthesis in the treatments with DHAs or the combinations of CNT/MCNTs and DHAs alleviated Phe-induced phytotoxicity and negative impacts on photosynthesis. Our findings provide important information on Phe accumulation and its metabolism in plant-soil systems and on the roles of DHAs and MCNTs in alleviating the contaminant-induced phytotoxicity.

Keywords: phenanthrene; magnetic carbon nanotubes; dissolved humic acids;

phenanthrene metabolites; phytotoxicity

Introduction

Polycyclic aromatic hydrocarbons (PAHs) are produced by the incomplete combustion of coal, petroleum and wood, etc. [1-3], and are ubiquitous contaminants in the environment, including the atmosphere, water, sediments, and soil.[4, 5] Due to their lipophilic and hydrophobic properties, PAHs are readily accumulated by terrestrial plants [6] and transfer via food chains in environment. Phenanthrene (Phe), a low-molecular weight PAHs with three benzene rings and representative structure with K region and bay region, has often been selected as a model compound to investigate the environmental behavior of PAHs.[7-9] Phe has been found in many fruits and vegetables, including Chinese cabbage (*Brassica rapa* L.), lettuce (*Lactuca sativa* L.), hibiscus (*Hibiscus syriacus* L.) and amaranth (*Amaranthus mangostanus* L.), with concentrations up to 2.0 mg/kg (dry weight).[10, 11] Besides, Phe exerted significant carcinogenic and mutagenic toxicity to organisms.[12] Therefore, investigations on uptake and metabolism of Phe in vegetables are of importance and provide useful information for phytoremediation in terrestrial ecosystems, including agricultural lands.

Carbon nanotubes (CNTs) have gained considerable attention because of their excellent mechanical, electrical, optical, and physicochemical properties.[13] Considering their large surface area and *p-p* electrostatic interactions, CNTs have shown significant potential for the adsorption of heavy metals [14-16] and organic pollutants [17, 18] as part of novel environmental remediation strategies. However, it is difficult to separate CNTs from water or soil matrices due to their nanoscale size. To overcome this disadvantage, CNTs can be decorated with magnetic nanoparticles such as Fe_3O_4 and Mn_2O, which can be enable facile separation from complex matrices as a novel strategy for soil remediation.[19, 20] It is highly likely that magnetic CNTs (MCNTs) will interact with PAHs in water or soil [21, 22], and may subsequently affect the physiological responses of plants, including PAH uptake. The important role of CNTs and other carbons (e.g. soot, charcoal) in lowering the bioavailability of contaminants has been demonstrated previously.[23-26] For example, biochar, charcoal, and activated carbon reduced the freely dissolved concentration (C_{free}) of six polybrominated diphenyl ethers (PBDEs) by 47.5–78.0%, 47.3–77.5%, and 94.1–98.3%, respectively.[23] Similarly, charcoal significantly reduced the bioaccumulation of 3,3',4,4'-tetrachlorobiphenyl and benzo[*a*]pyrene by the oligochaete (*Lumbriculus variegatus*).[24] However, investigation on effects of MCNTs on accumulation and metabolites of persistent organic pollutants (POPs) in plants is still largely unknown.

Humic acids (HAs) contain carboxyl, hydroxyl, phenolic and other active groups and are among the most active components in soil.[27, 28] HAs can affect hydrophobic organic contaminant (HOCs) speciation, transfer, and bioavailability.[29-31] For example, the relative distribution of terrestrial humic-like fluorophores was correlated with the extent of Phe binding ($r=0.571$; $p < 0.05$), suggesting that the presence of HAs enhanced the Phe binding affinity.[32] Conversely, Yang et al. (2014) reported that pine needle litter-derived DOM (dissolved organic matter, fulvic acid and humic acid) inhibited PAH sorption and promoted desorption.[33] DOM was shown to promote pyrene bioavailability to *Daphnia magna* when the C_{free} of pyrene was kept constant, and the bioavailability was related to DOM molecular weight.[34] Hence, the properties of DOM affect the speciation, transfer and bioavailability of HOCs. Our previous study also demonstrated that different classes of dissolved humic acid altered the uptake of hexabrominated diphenyl ether (BDE-153, a typical HOCs belonged to PBDEs) by *Lactuca sativa*.[35] In addition, the presence of dissolved humic acids (DHAs) also reduced the Fe accumulation and lipid content in lettuce. It is worth noting that the distribution of BDE-153 was also dependent on the DHA classes.[35] Given the similarities among HOCs, the potential toxicity of PAHs, and the widespread occurrence of DHAs in environment, it is important to investigate the mechanisms by which different fractions of DHAs alter PAH uptake by plants, particularly upon co-exposure to the MCNTs as part of a novel contaminant remediation technology.

Humic acids may interact with CNTs in aqueous phase of the rhizosphere [36], and thus, we hypothesize that different fractions of DHAs combined with CNTs could alter the pattern of organic pollutant accumulation and phytotoxicity. Previous work has demonstrated that the extent of organic pollutant toxicity may be influenced by the presence of carbon-based nanomaterials (CNMs). For example, CNT amendments resulted in a significant increase in Phe toxicity to *Daphnia magna* when compared to Phe alone. [37] Upon exposure to 10 mg/L CNTs and 5 mg/L soot, diuron reduced the photosynthetic activity of *Chlorella vulgaris* by approximately 78% and 34%, respectively.[38] However, the role of DHAs in altering the interaction between organic pollutants and CNMs remains largely unknown.

In the present study, lettuce (*Lactuca sativa* L.) was chosen as a target plant to investigate whether co-exposure MCNTs and different fractions of DHAs could potentially alter the Phe accumulation pattern and its metabolites in plants. Different fractions of DHAs were extracted from a farmland soil near an electronic waste recycling plant in Jinghai county in Tianjin, China (116°46′30.07″ W, 38°49′22.55″ N). MCNTs were synthetized using alkaline precipitation method according to our previous method.[39] In order to exclude interference from the complex soil matrix and better understand the interaction of different analytes, the plant exposure was conducted in hydroponic systems. Lettuce seedlings were exposed to Phe, DHAs, CNTs and MCNTs for 10 days. At harvest, Phe and its metabolites, and Fe were measured in lettuce across all the treatments. The activity of antioxidant enzymes and chlorophyll fluorescence were measured, and the transcription level of genes associated with photosynthesis and carotenoids synthesis were analyzed. Our findings provide useful information for phytoremediation of PAH contaminated soil using MCNTs.

MATERIALS AND METHODS

Chemicals and materials

Radioactive Phe (^{14}C-labeled Phe, 8.2 μCi/μmol) and unlabeled Phe were purchased from Sigma-Aldrich Chemical Co. and CNW Technology Inc., respectively. CNTs (95% purity, 20–30 nm outer diameter, 10–30 μm length) were purchased from Xianfeng Nano Material Co. Ltd., China. CNTs were acidified prior to loading with Fe to create MCNTs as described previously [39]; detailed methods are given in the supporting information (**SI**). CNTs and MCNTs were observed by transmission electron microscopy (TEM, **Figure S1**) (JEM-1230, JEOL, Ltd., Japan). Different fractions of DHAs (DHA1 and DHA4) were extracted from the surface soil (0-20 cm deep) of a farmland near an electronic waste recycling plant located in Jinghai county in Tianjin, China (116° 46′ 30.07″ W, 38° 49′ 22.55″ N). Detailed information on DHAs characterization was reported previously.[35, 39]

Experimental design

Lettuce seedlings were prepared according to Ma et al. (2016). [40] Briefly, lettuce seeds were sterilized by 70% ethanol and then germinated on moist filter paper. After growing in half-strength Hoagland's solution for 20 days (22/18 °C, 14/8 h, day/night), uniform-sized lettuce seedlings were selected for the hydroponic exposure. ^{14}C-labeled and unlabeled Phe were dissolved and mixed homogeneously in methanol as stock solution. Each lettuce seedling was grown in 230 mL Hoagland's solution with Phe at 1 mg/L, which was also amended with/without 10 mg/L DHAs and 25 mg/L CNTs/MCNTs for 10 days. Seedlings grown in the pure Hoagland's solution were set as the control. Others included Phe (P), carbon nanotubes (C), magnetic carbon nanotubes (M), and different fractions of DHA (H1 and H4). Details for each treatment are listed in **Table S1**. There were three biological replicates in each treatment. Air was pumped into the solution (14 h per day) to maintain a homogeneous mixture and provide oxygen for root respiration. At harvest, 30-day old seedlings were rinsed with deionized H_2O and weighted across all the treatments. Chlorophyll fluorescence was measured by Imaging-PAM (Walz Ltd., Germany). All plant tissues were stored at −80 °C (DW-86L388A, Qingdao Haier Electric Appliance Co., Ltd., China) until further analysis.

Phe extraction and measurement

Procedures for Phe extraction from plant tissues were described in Hadibarata et al. (2011) [41] and Gao et al. (2004) [42] with some modifications. One hundred milligrams of freeze-dried plant powders were ultrasonically extracted with 5 mL ethyl acetate for 1 hour at ambient temperature. This step was repeated three times and all extracts were combined and purified by silica gel column. The detailed sample cleanup procedures are given in SI. The extracts were then concentrated under nitrogen. One milliliter methanol was added to the dried plant residues and vortexed vigorously, waiting for the determination of Phe. To test the recovery rate of the Phe measurement, the Phe-free plant samples were homogeneously spiked with different concentrations of Phe at 5, 10 and 50 μg/g. All treated samples were stabilized overnight, then extracted and purified by the above method. The average recovery rate was between 81.7 and 94.3%, which satisfied the requirements for the Phe measurement in plant tissues.

An Agilent 1200 HPLC with fluorescence detector (Agilent 1200, Agilent Technologies, Inc.) was used to quantify the Phe concentration. A Symmetry C18 column (3.9 mm×150 mm, Waters) was employed as the stationary phase. The mobile phase was a mixture of methanol and ultrapure water (90:10, *v/v*) and delivered in a gradient program at speed of 0.9 mL/min. Identification and quantification were carried out using fluorescence detection with excitation wavelength at 250 nm and emission wavelength at 364 nm. A fitted eight-point calibration curve (r^2=0.998) was used for the Phe quantification. The limit of detection (LOD) of phenanthrene was 10 μg/L. The calculation formula was LOD = 3.14 × SD. SD is the standard deviation of repeat determination of a low concentration of Phe standard solution for seven times. In addition, the concentrations of Phe in the control plants were below the LOD.

Phe metabolites measurement

Quantification of Phe metabolites One hundred microliters of Phe-methanol solution were diluted to 1 mL with methanol and the mixture was added into 8 mL of Ultima Gold XR cocktail (Perkin-Elmer) for liquid scintillation counting (Beckman LS6500).[43, 44] ^{14}C-labled Phe and its metabolites was measured. The accuracy of the quantification of the total content of Phe metabolites were calculated directly by mass difference between Phe (including the metabolic Phe) determined by liquid scintillation and Phe determined by HPLC. Because of the ^{14}C-labeled Phe used in hydroponic experiment, the Phe that was taken up or metabolized by plants can be determined by their final radioactivity.

Qualitative analysis of Phe metabolites One hundred microliters of N,O-*bis*-trimethylsilyl acetamide and 50 μL of trimethylchlorosilane were added to the dried residues prior to heating at 60 °C for 1 h in a water bath. Analysis of the trimethylsilyl derivatives was performed on an Agilent 7890B (Agilent Technologies, USA) gas chromatograph equipped with a single quadrupole mass analyzer 5977B MSD. One microliter of derivatives solution was injected onto a DB-5ms column (J&W Scientific, 30 m × 0.25 mm i.d. × 0.25 μm film thickness) in splitless mode. Helium was used as carrier at a constant flow of 1.0 mL/min. The oven program started at 100 ℃ and held for 1 min, increased at 5 ℃/min to 200 ℃ and held for 5 min, then at 10 ℃/min to 300 ℃, and held for 10 min. The GC-MS (EI) was used in scan mode with a mass range from 50 – 450 m/z. The temperature of the EI and MS were 250 and 150 ℃, respectively. The mass spectrum of individual total ion peaks was identified by comparison with the NIST mass spectra database and main fragment ions according to literature review and database of Phe metabolic pathways.[41, 45, 46] The metabolites were also semi-quantitatively determined by the relative peak intensity.[47] **Table S2** lists the nine Phe metabolites identified in the plant samples.

Fe measurement in lettuce tissues

All root and shoot tissues were dried and weighed into sample tubes for acid digestion. Briefly, 6 mL of HNO_3 and 2 mL of H_2O_2 were added into each sample and the samples digested in a microwave chemical reactor (MDS-86, Shanghai Sineo Microwave Chemical Technology Co., Ltd). The digesting program was 140 °C for 7 min and then held at 180 °C for 15 min. The Fe content was measured by a continuum source atomic absorption spectrometer (Analytic Jena, contrAA 700, Germany).[48] To ensure the quality of the process, yttrium was used as an internal standard and a sample of known concentration was read every thirty samples.

Antioxidant enzymes and photosynthesis measurement

Enzymes were extracted in pre-chilled 50 mmol/L phosphate buffer (pH 7.5) containing 1 mmol/L ethylenediaminetetraacetic acid (EDTA) and 1 mmol/L dithiothreitol (DTT). The mixture was centrifuged at 10,000 *g* and the supernatant was collected for the measurement of enzyme activity. For the glutathione S-transferase (GST) activity measurement [40], 1-Chloro-2,4-dinitrobenzene (CDNB) was used as the reaction solution and the increase of absorbance was recorded at 340 nm for 5 min by a UV−Vis spectrophotometer (TU-1810, Persee, China). Catalase (CAT) and peroxidase (POD) activities were measured according to Beauchamp and Fridovich (1971) [49] and Aebi (1984).[50]

Chlorophyll fluorescence was measured using IMAGING-PAM (Walz Ltd., Germany), according to Erhard et al. (2008).[51] Details for photosynthesis measurement are provided in the **SI**.[48]

Gene regulation measurement by qRT-PCR

Lettuce shoot and root tissues were separately homogenized to fine powder in liquid nitrogen. Protocols for total RNA isolation, cDNA synthesis, and gene expression using qRT-PCR were described in Ma et al. (2013).[52] Briefly, a Spectrum™ plant total RNA kit (Sigma-Aldrich) was used to isolate total RNA, with the concentration being quantified by NanoDrop spectrophotometry (ThermoScientific, West Palm Beach, FL). A Verso cDNA synthesis kit (ThermoFisher Scientific) was used to synthesize cDNA and the gene-specific primers were designed using Primer Quest (Integrated DNA Technologies, Coralville, IA). Reverse-transcription real-time

PCR was performed with Bio-Rad SsoAdvanced Universal SYBR Green Supermix (Bio-Rad). A complete list of primer sequences is provided in **Table S3**. The PCR amplification program was: 95 °C for 30 s; 95 °C for 15 s, 63 °C for 30 s, repeating 40 cycles; melting curve from 65 °C to 95 °C. Relative quantities ($2^{-\Delta\Delta Ct}$ method) were used to calculate the transcription level of each gene.

Statistical analysis

A one-way analysis of variance (One-way ANOVA) followed by Duncan's multiple comparison test (IBM SPSS Statistics 20) was used to determine statistical significance of differences in each parameter across all treatments. The exception was the qRT-PCR assay, in which Student t-test was applied to determine statistical significance of the levels of each gene. In figures and tables, values followed by different letters are significantly different at $p < 0.05$.

RESULTS AND DISCUSSION

DHA characterization

Our previous studies indicated that differences on the element composition and physicochemical properties of DHA1 and DHA4 potentially affected the Phe behavior and physiological responses of plant.[35, 39] The moieties of humic acids are important contributors to determine the state of humic acids, in which aromatic moieties contribute to form the condensed state of humic acids, while aliphatic moieties are a contributor to form the expanded state.[43, 53, 54] According to the ^{13}C -NMR spectra of two types of humic acids [35], the DHA1 has a higher aromatic carbon content

(40.0%) and a lower aliphatic carbon content (11.1%) in comparison with DHA4, in which aromatic carbon and aliphatic carbon content was 32.1% and 29.3%, respectively. Therefore, DHA4 had higher partition capacities for Phe adsorption.[43] Additionally, DHA4 could bind minerals more tightly relative to DHA1.[17]

Phe and its metabolites in lettuce

Phe content The addition of CNTs/MCNTs and DHAs significantly decreased the content of Phe and its metabolites in lettuce roots by 16.5-86.1% as compared to the Phe alone treatment, except for treatments with CNTs and co-exposure of CNTs with DHA1 (**Figure 1A**). It is reported that CNTs could physically damage the plant cell walls and subsequently increase the contaminant uptake by roots.[55] Additionally, DHA1, containing more aromatic moieties in a condensed state, could decrease the Phe partition capacity and consequently increase its bioavailability to plants. Thus, the treatments of different fractions of DHA combined with CNTs resulted in different patterns of Phe uptake by roots. It is worth noting that MCNTs decreased the content of Phe and its metabolites; upon co-exposure to MCNTs and DHAs, the maximum decreases in the Phe and metabolite content were evident. The hydrophobic CNTs functionalized with nano-sized iron oxide could disperse better in water with an increasing specific surface area [56], and therefore the adsorption capacity of the modified CNTs became higher than that of the pure CNTs. In addition, the presence of different fractions of DHAs could further increase the sorption of nano-sized iron oxides to the hydrophobic organic compounds.[17] The complexation of MCNTs and

DHAs increased the MCNTs dispersion in a more expanded state, and more adsorptive sites could be exposed to bind with Phe. Overall, the high adsorption capacity of MCNTs combined with DHAs could effectively inhibit the Phe uptake by lettuce.

Without considering the metabolic Phe, in lettuce roots, the presence of MCNTs and the combination with different fractions of DHA decreased the root Phe content by more than 50% relative to the Phe alone treatment (**Figure 1B**). The co-exposure of CNTs and DHA1 increased the root Phe content as compared to the Phe alone treatment. In shoots, a common finding was that the addition of CNTs increased the Phe accumulation to the aboveground tissues by 72.1-114.8% when compared to the Phe alone treatment, regardless of the DHA amendments. Although the Phe accumulation as affected by MCNTs was largely similar to the CNT treatments, the increase was smaller by 11.5-98.4 % compared to the increase with CNTs (**Figure 1B**). It could be ascribed as that much less Phe accumulation in MCNTs treated roots than that in CNTs treated ones resulted in relatively low translocation of Phe from roots to the aboveground parts.

The translocation factor of Phe (TF_{Phe}) from roots to shoots shows that DHAs had no impact on the Phe translocation as compared to the Phe alone treatment (**Figure 1C**). However, the addition of CNTs and MCNTs significantly increased TF_{Phe} by 54.0-220.9%, regardless of the DHA addition. Our previous study reported that some black granules appeared around the protoplasts in shoot and root cells, indicating the presence of iron particles or magnetic CNTs.[39] An increasing numbers of studies reported the CNT uptake by plants [56-60], and hence enhancing the transportation of CNT carried environmental toxins into living cells.[61] Therefore, the Phe translocation in lettuce might be elevated by the CNTs/MCNTs due to the Phe adsportion on CNTs/MCNTs. Additionally, although adding DHAs potentially increased the Phe translocation, the statistical analysis indicates otherwise due to the large variability (**Figure 1C**). A possible explanation that MCNTs significantly elevated TF_{Phe} as compared to CNTs might be that the functionalized CNTs could enter plants cells more easily in comparison with the pure CNTs.[56]

Total Phe metabolite content CNTs/MCNTs and DHAs significantly decreased the content of Phe metabolites in lettuce roots from 18.4% to 98.9% as compared to the Phe alone, the exception were the treatments of MCNTs and co-exposure of CNTs with DHA1 (**Figure 1D**), where the root Phe metabolite content was equivalent to the Phe alone treatment. In lettuce shoots, all the treatments significantly decreased the content of Phe metabolites from 21.7% to 88.6% as compared to the Phe alone, except for CNT and MCNT treatments. The metabolites were further analyzed by the ratio of the total metabolites to the Phe content in lettuce (**Figure 1E**). It was found that the ratios of the total metabolites to the Phe content in lettuce were all significantly decreased as compared to the Phe alone treatment by 23.8% to 97.1%, except for the ratio in roots co-treated with Phe and MCNTs, which was significantly higher by 131% compared with other treatments (**Figure 1E**). Besides, the combination of DHAs with CNTs/MCNTs exerted stronger inhibition on Phe metabolites ratio than CNTs/MCNTs alone both in roots and shoots in rough. For example, DHAs combined with CNTs decreased the Phe metabolites ratio by more than 11.5% in relative to CNTs alone; DHAs combined with MCNTs decreased the Phe metabolites ratio by more than 67.0% in relative to MCNTs alone. DHAs play an important role in inhibiting the Phe metabolism in lettuce, while MCNTs can facilitate this process. In DHA treatments, the complexing form of Phe with DHAs was also taken up by lettuce. Therefore, less Phe were bioavailable to metabolic enzymes because of hydrophobic interaction with DHAs, as well as the potential π-bonds of Phe with aromatic moieties of DHAs.[43] In addition, the presence of DHAs also resulted in agglomeration of CNTs/MCNTs, which blocked CNMs penetrating into the plant cells. Given that CNMs could potentially adsorbed Phe, less CNMs in living cells consequently lowered the Phe accumulation and metabolites. X-ray spectra of CNTs/MCNTs demonstrated that 1.93% of Fe were detected on the MCNTs surface, which including 44% Fe(II) (710.8 eV binding energy) and 56% Fe(III) (712.5 eV).[39] The iron oxides coated onto carbon materials were consisted of magnetite, Fe_3O_4, maghemite and γ-Fe_2O_3.[62-64] Iron oxides, as electron shuttles, can elevate electron transfer from iron-reducing or dehalogenating bacteria to PAHs, subsequently increasing the degradation rate of PAHs.[65] Additionally, cytochrome P450, a ubiquitous superfamily of mixed function detoxifying oxidases, belongs to Fe containing hemoprotein.[66-68] Thus, it is reasonable to speculate that the Fe released from MCNTs might stimulate the Phe metabolism by inducing the cytochrome P450 activity.

Metabolite profile of Phe

The content of Phe metabolites varied between lettuce roots and shoots across all the treatments (**Figure 2**). Nine Phe metabolites were identified in lettuce tissues, and the majority were produced by oxygen-addition that facilitated ring opening. The detected metabolites were trans-2, 3-dioxo-5-(2'-hydroxyphenyl)-pent-4-enoic acid (metabolite A), phthalic acid (metabolite B), salicylic acid (metabolite C), protocatechuic acid (metabolite D), 2,4-dihyoxybenzoicacid (metabolite E), 2,3-dihyoxybenzoicacid (metabolite F), p-hydroxy benzoic acid (metabolite G), 3-hydroxybenzoic acid (metabolite H) and benzoic acid (metabolite I). With regard to treatment effects, MCNTs+DHAs+Phe significantly decreased the content of metabolites in both shoots and roots, which is consistent with the total metabolite analysis (**Figure 1B**). Conversely, in the CNT treatments, the addition of both DHAs notably increased the content of metabolites A, B, D, G, and H (**Figure 2**). Thus, it is clear that co-exposure to DHAs and MCNTs impacts the Phe metabolism in lettuce tissues.

In the present work, we were able to identify numerous intermediate Phe metabolites in lettuce seedlings by comparing with the previous studies.[45, 69, 70] However, the potential metabolic pathways of Phe in plants are still unknown. Thus, we proposed a possible Phe metabolism pathway in lettuce by referencing characterized pathways in microorganisms. *Mycobacterium vanbaaleni*i PYR-1 was capable of degrading Phe to ring cleavage metabolites such as 1-hydroxy-2-naphthoic, suggesting that multiple dioxygenases and monooxygenases might be involved in Phe biodegradation.[71-73] The metabolite 1-hydroxy-2-naphthoic could be further degraded into metabolite B and metabolite C by the phthalic acid and naphthalene pathways, respectively.[73] Given the identified Phe metabolites, we proposed metabolic pathways of Phe through metabolite B and metabolite C to downstream metabolites (**Figure S2**). Salicylaldehyde, produced by the reduction of metabolite A via hydratase-aldolase, further degraded into metabolite C through the action of aldehyde dehydrogenase.[46] Metabolite B could also degrade into metabolite C by hydroxylase. Subsequently, metabolite C could be metabolized into salicylic acid 3,4-dihydrodiol by dioxygenase, and further degraded into metabolites D-I via dehydrogenase activity (**Figure S2**).

Biomass

Exposure to Phe alone resulted in an approximately 23.4% decrease as compared to the control (**Figure S3**). In the presence of DHA1, the dry weight of Phe treated lettuce was close to the Phe alone treatment; while approximately 23.1 and 60.8% increase in dry weight of Phe treated lettuce upon exposure to DHA4 were evident when comparing to the control and the Phe alone treatment, respectively (**Figure S3**). In addition, co-exposure to MCNTs and Phe also significantly decreased the total dry biomass by 23.3%, which was similar to the Phe alone treatment. DHA4 performed better on increasing the Phe treated lettuce biomass than DHA1 treated ones, probably because of the higher content of Phe metabolites in DHA1 treated lettuce (**Figure 1D**). Metabolized Phe with more hydrophilic structures became electrophilic, and could bind with cellular macromolecules such as DNA, forming PAH-DNA adducts.[74] Therefore, the Phe metabolites could usually cause more toxicity to plants than Phe itself, and exert a more negative impact on plant growth. However, the lettuce biomass was not just affected by the content of Phe metabolites. CNTs aciting as a growth inducer [58, 75] might be able to counteract the toxicity induced by the Phe metabolites. For example, 28.5-50.6% increase in lettuce biomass was evident in CNT, CNTs+DHA1, and CNTs+DHA4 treatments as compared to the Phe alone treatment. In addition to the DHA4 alone treatment, the combination of DHAs and CNTs/MCNTs also alleviated the adverse effects of Phe on plant biomass, especially for the treatment with co-exposure of MCNTs and DHA4.

Fe content

A common finding for the Fe accumulation was that the presence of CNTs/MCNTs decreased the root Fe content (**Figure 3A**). In shoots, co-exposure to MCNTs and Phe increased the Fe content by approximately 50% as compared to the control and the Phe alone treatment (**Figure 3B**). A decreasing trend was evident in the DHAs+MCNTs+Phe treatment when comparing with the one co-treated with MCNTs and Phe, suggesting that DHAs complexed with MCNTs and subsequently inhibited the Fe release from MCNTs. The correlation (r^2) between the Fe and the Phe content in lettuce indicates that the addition of different fractions of DHAs did alter the relationship between the Fe and the Phe uptake by lettuce treated with MCNTs/CNTs (**Figure 3C-H**).

The presence of DHA1 altered the correlation between Fe and Phe. The Fe content in both lettuce shoots and roots was positively correlated with the Phe, with a r^2 at 0.864

and 0.681, respectively (**Figure 3F**). Our previous results of DHA characterization suggested that the aliphatic C content of DHA1 and DHA4 was 11.1 and 29.3%, respectively; the aromatic C content of DHA1 and DHA4 was 30.8 and 21.4%, respectively.[35] As a result, a higher aromaticity of DHA1 might contribute to the positive correlation between the Fe and the Phe translocation in lettuce. One possible explanation could be that DHAs as colloidal suspensions in nutrient solution controlled the oxidation rate of Fe (II) and maintained Fe (III) (hydr)oxides in natural waters.[76] This occurred along with complexation of Fe and Phe, which eventually contributed to the correlation between these two analytes in lettuce. Besides, the DHA4 with a higher content of aliphatic C bound more tightly to Fe minerals might consequently interfere the positive correlation between the Phe and the Fe content in lettuce.[77]

Antioxidant enzymes activity

Antioxidant defense systems in plants play a central role in the detoxification of xenobiotic compounds and of scavenging reactive oxygen species (ROS).[78] In the Phe treatment, CAT activity in both roots and shoots was unaltered as compared to the control (**Figure 4 A and B**). The addition of DHA1 and DHA4 increased root CAT activity by 3- and 4-fold relative to the control, respectively; similar findings were evident in the MCNTs and Phe co-treated roots (**Figure 4A**). However, in the shoots only the DHA1+MCNTs+Phe treatment significantly increased the CAT activity by approximately 60% as compared to the control. The other treatments had no impact on the CAT activity. The root POD activity was largely unaffected treatment, with the exception being MCNTs+Phe, where the root POD was 2.8-fold that of the control (**Figure 4C**). In the shoots, the addition of Phe dramatically elevated the POD activity as compared to the control (**Figure 4D**); however, the presence of CNMs or different fractions of DHAs, significantly reduced the shoot POD levels. The GST activity in both roots and shoots was significantly decreased in the Phe alone treatment (**Figure 4 E and F**). It is worth noting that the addition of MCNTs, CNTs or different types of DHAs restored GST levels to that of the control in roots. The GST activities in shoots were also significantly increased by adding exogenous materials as compared to the Phe alone treatment. The co-exposure of DHA1 and Phe even increased the GST activities by 46.9% as compared to the control. Song et al. (2012) reported that the addition of pyrene significantly increased the shoot CAT activity and root POD activity in mangrove.[79] The GST activity was also increased significantly in wheat leaves that were treated with 1.0 mg/L Phe for 5 days.[80]

Upon exposure to Phe, the shoot POD activity was significantly increased, suggesting that the contaminant may have triggered H_2O_2 accumulation in shoots. Decreases in the shoot POD activity in the presence of DHAs and CNMs further confirm that both analytes significantly alleviated the Phe-induced stresses, including reducing H_2O_2 generation in lettuce. Co-exposure of Phe and DHA1 led to a more notable decrease in the POD activity as compared to the combination of Phe and DHA4. In addition, decreases in the GST activity in the Phe alone treatment suggest that the generation of GST-Phe conjugates as intermediate metabolites was inhibited. However, the addition of MCNTs/CNTs and DHAs restored the GST activity back to the control level or even higher levels when treating with DHA1. The variation of POD and GST activity suggesting that both MCNTs/CNTs and DHAs could alleviate Phe-induced toxicity, especially DHA1.

Chlorophyll fluorescence

The maximum quantum efficiency (F_v/F_m) represents the intrinsic photosynthetic efficiency of photosystem II (PSII) [81], and is a strong indicator to abiotic and biotic stress.[82] The single or co-treatments of Phe, CNTs and DHAs had no impact on photosynthetic efficiency, the exception being co-treatment of DHA1, CNTs and Phe, in which a 25% decrease was evident as compared to the control (**Figure 5A**). However, the swamp model (qP) and the Lake model (qL) were both used to calculate the intensity of the photochemical quenching coefficient (**Figure 5B and C**). Both qP and qL show a similar trend as affected by Phe alone, or with co-treatments of CNTs and DHAs; both CNTs and MCNTs significantly increased qP and qL by 20 and 50%, respectively. Similarly, in the three analyte-combined treatments, increases in both qP and qL were also evident as compared to the control. The intensity of the photochemical quenching coefficient represented by qP and qL can be used as an estimate of the fraction of 'open' PSII centers (with QA oxidized) and therefore reflects the intensity of photosynthetic activity.[83] Therefore, CNMs alone, as well as the combination of DHAs and MCNTs, could potentially enhance photosynthesis. However, the classes of DHAs had no impact on both qP and qL. Besides, no difference was evident on the non-regulatory energy dissipation coefficient (Y(NO)), the exception being treatment with DHA1+CNTs+Phe, in which Y(NO) was significantly higher as compared to the control and Phe-alone treatment (**Figure 5D**). The higher the value of Y (NO), the more likely the plants would suffer from light stress.[84]

Transcriptomics

Cytochrome b6 (petB) mediates electron transfer between photosystem II (PSII) and PSI.[85] Two additional genes, PSII D1 protein (psbA) and PSII CP43 reaction center protein (PSII light-harvesting protein, psbC) [86], in the PSII reaction center were analyzed as a function of treatment. The relative expression of all three genes displayed a similar pattern across treatments with Phe, CNTs/MCNTs, and DHA1/DHA4 (**Figure 6A-C**). In the Phe or Phe+CNT/MCNT treatments, significant downregulation (60-70% less) of all three genes was evident as compared to the control. Although the addition of MCNTs showed the less impact as compared to the CNT treatment, the relative expression was still quite low. However, the addition of DHA1 and DHA4 significantly elevated the relative expression of petB, psbA and psbC by approximately 56-70%, 20-30%, and 37-48%, respectively, as compared to the corresponding Phe alone treatment. In addition, the presence of MCNTs and DHAs restored the relative expression of all the three genes back to the control level, suggesting that the combination of MCNTs and DHAs might exert an important role in alleviating the contaminant-induced negative impacts on photosynthetic systems.

The carotenoid biosynthesis pathway is a secondary metabolic pathway in the chloroplast, and carotenoid compounds play important roles in regulating hormones, pigments and volatile organic compounds.[87] Two types of carotenoid dioxygenases have been identified, including carotenoid cleavage dioxygenase (CCDs) and 9-cis-epoxycarotenoid cleavage dioxygenases (NCEDs).[88] As shown in **Figure 6D and E**, the relative expression of CCD1 and NCED1 was 45% and 78% that of the control, respectively. Similar results were evident upon treatment with CNTs and Phe. However, the addition of MCNTs restored the expression of both genes back to the control level. Additionally, upon exposure to the combination of all three analytes, the relative expression of CCD1 was nearly 2-fold that of the control; the NCED1 expression was restored to the control level. Overall, the above results again demonstrate that different fractions of DHAs in conjunction with CNTs/MCNTs can significantly alleviate Phe-induced phytotoxicity to lettuce. Two carotenoid related genes were also altered by Phe, CNTs/MCNTs, and DHAs. The CCDs are involved in plant growth and development and NCEDs can regulate phytohormone levels (e.g. abscisic acid).[89] Co-exposure to CNMs and DHAs significantly up-regulated both genes to levels that were equivalent to controls or higher, again demonstrating that both analytes could counteract Phe-induced abiotic stresses.

In summary, one of the main findings was that the addition of CNTs/MCNTs and DHAs decreased the total Phe and its metabolites content in lettuce roots. However, the performance of the functionalized nano-iron oxide coated MCNTs on altering the accumulation and translocation was distinguished from the pure CNTs. It is worth noting that a positive correlation between the Fe and the Phe content in lettuce was evident in the treatments with DHA1+MCNTs/CNTs. DHAs played an important role in inhibiting the Phe metabolism in lettuce, while MCNTs facilitated this process. Additionally, co-exposure to MCNTs/CNTs and DHAs reduced the Phe-induced toxicity to lettuce as determined by the increases in the GST activity and the elevated photosynthetic efficiency. The overall results could provide important information for the Phe and its metabolisms in lettuce as affected by MCNTs/CNTs and DHAs.

Supporting information

Procedures for the synthesis of magnetic CNTs and photosynthesis analysis are provided in the supporting information (SI). Additional information on magnetic carbon nanotube characterization, lettuce dry biomass, proposed metabolic pathways of Phe, details of experimental design, Phe metabolites, and a list of gene primers is also given in the SI.

Acknowledgments

This work was supported by the Natural Science Foundation of China (41673104) and Ministry of Science and Technology of China (2014CB441104) and Tianjin Science and Technology Committee (17JCZDJC39600), and the Fundamental Research Funds for the Central Universities and 111 program, Ministry of Education, China (T2017002) and Tianjin Agricultural Affair Committee, China (201604010) and USDA NIFA McIntire-Stennis and Hatch Program (MAS 00028 and CONH00147, respectively) .

References

[1] Singh P, Sung C-J. PAH formation in counterflow non-premixed flames of butane and butanol isomers. Combustion and Flame 2016;170:91-110.
[2] Choi SK, Choi BC, Lee SM, Choi JH. The effect of liquid fuel doping on PAH and soot formation in counterflow ethylene diffusion flames. Experimental Thermal and Fluid Science 2015;60:123-31.
[3] Wiersum UE. The Formation of Polycyclic Aromatics, Fullerenes and Soot in Combustion. The Mechanism and the Environmental Connection. Polycyclic Aromatic Compounds 1996;11:291-300.
[4] Hao Y, Fang P, Ma C, White JC, Xiang Z, Wang H, et al. Engineered nanomaterials inhibit Podosphaera pannosa infection on rose leaves by regulating phytohormones. Environmental research 2019;170:1-6.
[5] Qu C, Albanese S, Lima A, Hope D, Pond P, Fortelli A, et al. The occurrence of OCPs, PCBs, and PAHs in the soil, air, and bulk deposition of the Naples metropolitan area, southern Italy: Implications for sources and environmental processes. Environ Int 2019;124:89-97.
[6] Jia J, Bi C, Zhang J, Jin X, Chen Z. Characterization of polycyclic aromatic hydrocarbons (PAHs) in vegetables near industrial areas of Shanghai, China: Sources, exposure, and cancer risk. Environ Pollut 2018;241:750-8.
[7] Chen S, Ma Z, Li S, Waigi MG, Jiang J, Liu J, et al. Colonization of polycyclic aromatic hydrocarbon-degrading bacteria on roots reduces the risk of PAH contamination in vegetables. Environ Int 2019;132.
[8] Wang J, Liu X, Liu G, Zhang Z, Wu H, Cui B, et al. Size effect of polystyrene microplastics on sorption of phenanthrene and nitrobenzene. Ecotoxicology and Environmental Safety 2019;173:331-8.
[9] Ma Y, Huang A, Cao S, Sun F, Wang L, Guo H, et al. Effects of nanoplastics and microplastics on toxicity, bioaccumulation, and environmental fate of phenanthrene in fresh water. Environmental Pollution 2016;219:166-73.
[10] Mohammed S, Obiri S, Ansa-Asare OD, Dartey G, Kuddy R, Appiah S. Assessment of concentration of polycyclic aromatic hydrocarbons (PAHs) in vegetables from farms in Accra, Ghana. Environmental Monitoring and Assessment 2019;191.
[11] Paris A, Ledauphin J, Poinot P, Gaillard J-L. Polycyclic aromatic hydrocarbons in fruits and vegetables: Origin, analysis, and occurrence. Environmental Pollution 2018;234:96-106.
[12] Zhang Y, Tao S, Shen H, Ma J. Inhalation exposure to ambient polycyclic aromatic hydrocarbons and lung cancer risk of Chinese population. Proceedings of the National Academy of Sciences of the United States of America 2009;106:21063-7.
[13] Chang X, Henderson WM, Bouchard DC. Multiwalled carbon nanotube dispersion methods affect their aggregation, deposition, and biomarker response. Environ Sci Technol 2015;49:6645-53.

[14] Mubarak NM, Sahu JN, Abdullah EC, Jayakumar NS. Removal of Heavy Metals from Wastewater Using Carbon Nanotubes. Separation & Purification Methods 2014;43:311-38.
[15] Lu C, Chiu H. Adsorption of zinc(II) from water with purified carbon nanotubes. Chemical Engineering Science 2006;61:1138-45.
[16] Cho HH, Wepasnick K, Smith BA, Bangash FK, Fairbrother DH, Ball WP. Sorption of aqueous Zn[II] and Cd[II] by multiwall carbon nanotubes: the relative roles of oxygen-containing functional groups and graphenic carbon. Langmuir 2010;26:967-81.
[17] Yang K, Zhu L, Xing B. Adsorption of polycyclic aromatic hydrocarbons by carbon nanomaterials. Environmental Science & Technology 2006;40:1855-61.
[18] Zhang X, Kah M, Jonker MT, Hofmann T. Dispersion state and humic acids concentration-dependent sorption of pyrene to carbon nanotubes. Environ Sci Technol 2012;46:7166-73.
[19] Gui X, Zeng Z, Lin Z, Gan Q, Xiang R, Zhu Y, et al. Magnetic and highly recyclable macroporous carbon nanotubes for spilled oil sorption and separation. ACS applied materials & interfaces 2013;5:5845-50.
[20] Li S, Gong Y, Yang Y, He C, Hu L, Zhu L, et al. Recyclable CNTs/Fe3O4 magnetic nanocomposites as adsorbents to remove bisphenol A from water and their regeneration. Chemical Engineering Journal 2015;260:231-9.
[21] Menezes HC, de Barcelos SM, Macedo DF, Purceno AD, Machado BF, Teixeira AP, et al. Magnetic N-doped carbon nanotubes: A versatile and efficient material for the determination of polycyclic aromatic hydrocarbons in environmental water samples. Analytica chimica acta 2015;873:51-6.
[22] Moazzen M, Ahmadkhaniha R, Gorji ME, Yunesian M, Rastkari N. Magnetic solid-phase extraction based on magnetic multi-walled carbon nanotubes for the determination of polycyclic aromatic hydrocarbons in grilled meat samples. Talanta 2013;115:957-65.
[23] Jia F, Gan J. Comparing black carbon types in sequestering polybrominated diphenyl ethers (PBDEs) in sediments. Environ Pollut 2014;184:131-7.
[24] Pehkonen S, You J, Akkanen J, Kukkonen JV, Lydy MJ. Influence of black carbon and chemical planarity on bioavailability of sediment-associated contaminants. Environ Toxicol Chem 2010;29:1976-83.
[25] Schwab F, Camenzuli L, Knauer K, Nowack B, Magrez A, Sigg L, et al. Sorption kinetics and equilibrium of the herbicide diuron to carbon nanotubes or soot in absence and presence of algae. Environ Pollut 2014;192:147-53.
[26] Balasubramani A, Rifai HS. Efficacy of carbon-based materials for remediating polychlorinated biphenyls (PCBs) in sediment. Sci Total Environ 2018;644:398-405.
[27] Song J, Jin X, Wang XC, Jin P. Preferential binding properties of carboxyl and hydroxyl groups with aluminium salts for humic acid removal. Chemosphere 2019;234:478-87.
[28] SERUDO, Lima R, Oliveira DE, Camargo L, ROCHA, Cesar J, et al. Reduction capability of soil humic substances from the Rio Negro basin, Brazil, towards Hg(II) studied by a multimethod approach and principal component analysis (PCA).

Geoderma 2007;138:229-36.
[29] Huang W, Peng P, Yu Z, Fu J. Effects of organic matter heterogeneity on sorption and desorption of organic contaminants by soils and sediments. Applied Geochemistry 2003;18:955-72.
[30] Bohm L, Schlechtriem C, During RA. Sorption of Highly Hydrophobic Organic Chemicals to Organic Matter Relevant for Fish Bioconcentration Studies. Environ Sci Technol 2016;50:8316-23.
[31] Pan B, Ning P, Xing B. Part IV-sorption of hydrophobic organic contaminants. Environ Sci Pollut Res Int 2008;15:554-64.
[32] Hur J, Lee BM, Shin KH. Spectroscopic characterization of dissolved organic matter isolates from sediments and the association with phenanthrene binding affinity. Chemosphere 2014;111:450-7.
[33] Yang X-H, Garnier P, Wang S-Z, Bergheaud V, Huang X-F, Qiu R-L. PAHs sorption and desorption on soil influenced by pine needle litter-derived dissolved organic matter. Pedosphere 2014;24:575-84.
[34] Lin H, Xia X, Bi S, Jiang X, Wang H, Zhai Y, et al. Quantifying Bioavailability of Pyrene Associated with Dissolved Organic Matter of Various Molecular Weights to Daphnia magna. Environ Sci Technol 2018;52:644-53.
[35] Wang C, Ma C, Jia W, Wang D, Sun H, Xing B. Combined effects of dissolved humic acids and tourmaline on the accumulation of 2, 2', 4, 4', 5, 5'- hexabrominated diphenyl ether (BDE-153) in Lactuca sativa. Environmental pollution 2017;231:68-77.
[36] Wang F, Yao J, Yu C, Chen H, Yi Z, Choi MMF. Mutual Effects of Dialkyl Phthalate Esters and Humic Acid Sorption on Carbon Nanotubes in Aqueous Environments. ACS Sustainable Chemistry & Engineering 2014;2:1219-27.
[37] Zindler F, Glomstad B, Altin D, Liu J, Jenssen BM, Booth AM. Phenanthrene Bioavailability and Toxicity to Daphnia magna in the Presence of Carbon Nanotubes with Different Physicochemical Properties. Environ Sci Technol 2016;50:12446-54.
[38] Schwab F, Bucheli TD, Camenzuli L, Magrez A, Knauer K, Sigg L, et al. Diuron sorbed to carbon nanotubes exhibits enhanced toxicity to Chlorella vulgaris. Environ Sci Technol 2013;47:7012-9.
[39] Jia W, Zhai S, Ma C, Cao H, Wang C, Sun H, et al. The role of different fractions of humic acid in the physiological response of amaranth treated with magnetic carbon nanotubes. Ecotoxicology and Environmental Safety 2019;169:848-55.
[40] Ma C, Liu H, Guo H, Musante C, Coskun SH, Nelson BC, et al. Defense mechanisms and nutrient displacement in Arabidopsis thaliana upon exposure to CeO2 and In2O3 nanoparticles. Environmental Science: Nano 2016;3:1369-79.
[41] Hadibarata T, Tachibana S, Askari M. Identification of metabolites from phenanthrene oxidation by phenoloxidases and dioxygenases of polyporus sp. S133. J Microbiol Biotechnol 2011;21:299-304.
[42] Gao Y, Zhu L. Plant uptake, accumulation and translocation of phenanthrene and pyrene in soils. Chemosphere 2004;55:1169-78.
[43] Yang K, Xing B. Sorption of phenanthrene by humic acid-coated nanosized TiO2 and ZnO. Environ Sci Technol 2009;43:1845–51.
[44] Wang Z, Zhao J, Song L, Mashayekhi H, Chefetz B, Xing B. Adsorption and

Desorption of Phenanthrene on Carbon Nanotubes in Simulated Gastrointestinal Fluids. Environmental Science & Technology 2011;45:6018-24.
[45] Fu W, Xu M, Sun K, Hu L, Cao W. Biodegradation of phenanthrene by endophytic fungus Phomopsis liquidambari in vitro and in vivo. Chemosphere 2018;203:160-9.
[46] Stingley RL, Khan AA, Cerniglia CE. Molecular characterization of a phenanthrene degradation pathway in Mycobacterium vanbaalenii PYR-1. Biochemical & Biophysical Research Communications 2004;322:133-46.
[47] Luan TG, Yu KS, Zhong Y, Zhou HW, Lan CY, Tam NF. Study of metabolites from the degradation of polycyclic aromatic hydrocarbons (PAHs) by bacterial consortium enriched from mangrove sediments. Chemosphere 2006;65:2289-96.
[48] Jia W, Ma C, White JC, Yin M, Cao H, Wang J, et al. Effects of biochar on 2, 2′, 4, 4′, 5, 5′-hexabrominated diphenyl ether (BDE-153) fate in Amaranthus mangostanus L.: Accumulation, metabolite formation, and physiological response. Science of The Total Environment 2019;651:1154-65.
[49] Beauchamp C, Fridovich I. Superoxide dismutase: improved assays and an assay applicable to acrylamide gels. Anal Biochem 1971;44:276-87.
[50] Aebi H. Catalase in vitro. Methods Enzymol 1984;105:121-6.
[51] Erhard P, Christof K, Ulrich S. Monitoring the effects of reduced PSII antenna size on quantum yields of photosystems I and II using the Dual-PAM-100 measuring system. PAM Appl 2008;1:21-4.
[52] Ma C, Chhikara S, Xing B, Musante C, White JC, Dhankher OP. Physiological and molecular response of Arabidopsis thaliana (L.) to nanoparticle cerium and indium oxide exposure. ACS Sustainable Chemistry & Engineering 2013;1:768-78.
[53] Kang SH, Xing BS. Phenanthrene sorption to sequentially extracted soil humic acids and humins. Environmental Science & Technology 2005;39:134-40.
[54] Gunasekara AS, Xing BS. Sorption and desorption of naphthalene by soil organic matter: Importance of aromatic and aliphatic components. Journal of Environmental Quality 2003;32:240-6.
[55] Deng Y, Eitzer B, White JC, Xing B. Impact of multiwall carbon nanotubes on the accumulation and distribution of carbamazepine in collard greens (Brassica oleracea). Environmental Science-Nano 2017;4:149-59.
[56] Liné C, Larue C, Flahaut E. Carbon nanotubes: Impacts and behaviour in the terrestrial ecosystem - A review. Carbon 2017;123:767-85.
[57] Gogos A, Moll J, Klingenfuss F, van der Heijden M, Irin F, Green MJ, et al. Vertical transport and plant uptake of nanoparticles in a soil mesocosm experiment. Journal of Nanobiotechnology 2016;14.
[58] Vithanage M, Seneviratne M, Ahmad M, Sarkar B, Ok YS. Contrasting effects of engineered carbon nanotubes on plants: a review. Environmental geochemistry and health 2017;39:1421-39.
[59] Cano AM, Kohl K, Deleon S, Payton P, Irin F, Saed M, et al. Determination of uptake, accumulation, and stress effects in corn (Zea mays L.) grown in single-wall carbon nanotube contaminated soil. Chemosphere 2016;152:117-22.
[60] Zhai G, Gutowski SM, Walters KS, Yan B, Schnoor JL. Charge, Size, and Cellular Selectivity for Multiwall Carbon Nanotubes by Maize and Soybean. Environmental

Science & Technology 2015;49:7380-90.
[61] Wild E, Jones KC. Novel Method for the Direct Visualization of in Vivo Nanomaterials and Chemical Interactions in Plants. Environmental Science & Technology 2009;43:5290-4.
[62] Chen B, Chen Z, Lv S. A novel magnetic biochar efficiently sorbs organic pollutants and phosphate. Bioresource technology 2011;102:716-23.
[63] Han Z, Sani B, Mrozik W, Obst M, Beckingham B, Karapanagioti HK, et al. Magnetite impregnation effects on the sorbent properties of activated carbons and biochars. Water Research 2015;70:394-403.
[64] Kakavandi B, Jonidi A, Rezaei R, Nasseri S, Ameri A, Esrafily A. Synthesis and properties of Fe3O4-activated carbon magnetic nanoparticles for removal of aniline from aqueous solution: equilibrium, kinetic and thermodynamic studies. Iranian Journal of Environmental Health Science & Engineering 2013;10:1-9.
[65] Song M, Luo C, Li F, Jiang L, Wang Y, Zhang D, et al. Anaerobic degradation of Polychlorinated Biphenyls (PCBs) and Polychlorinated Biphenyls Ethers (PBDEs), and microbial community dynamics of electronic waste-contaminated soil. Science of the Total Environment 2015;502:426-33.
[66] Shimada T, Takenaka S, Murayama N, Kramlinger VM, Komori M. Oxidation of pyrene, 1-hydroxypyrene, 1-nitropyrene and 1-acetylpyrene by human cytochrome P450 2A13. Xenobiotica 2015;46:211.
[67] Im SC, Waskell L. The interaction of microsomal cytochrome P450 2B4 with its redox partners, cytochrome P450 reductase and cytochrome b5. Archives of Biochemistry & Biophysics 2011;507:144-53.
[68] a JBH, a JHH, a ALL, b JYW, a AD, a JNM. Zebrafish CYP1A expression in transgenic Caenorhabditis elegans protects from exposures to benzo[a]pyrene and a complex polycyclic aromatic hydrocarbon mixture. Toxicology 2020;440:152473.
[69] Zyakun AM, Kochetkov VV, Zakharchenko VN, Baskunov BP, Peshenko VP, Laurinavichius KS, et al. Application of High-Performance Liquid Chromatography/High Resolution Mass Spectrometry to the Investigation of the Biodegradation and Transformation of Phenanthrene by a Plasmid Bearing Rhizosphere Bacteria Pseudomonas aureofaciens. Journal of Analytical Chemistry 2019;74:1355-61.
[70] Sun K, Habteselassie MY, Liu J, Li S, Gao Y. Subcellular distribution and biotransformation of phenanthrene in pakchoi after inoculation with endophytic Pseudomonas sp as probed using HRMS coupled with isotope-labeling. Environmental Pollution 2018.
[71] Stingley RL, Khan AA, Cerniglia CE. Molecular characterization of a phenanthrene degradation pathway in Mycobacterium vanbaalenii PYR-1. Biochem Biophys Res Commun 2004;322:133-46.
[72] Fu W, Xu M, Sun K, Hu L, Cao W, Dai C, et al. Biodegradation of phenanthrene by endophytic fungus Phomopsis liquidambari in vitro and in vivo. Chemosphere 2018;203:160-9.
[73] Elyamine AM, Moussa MG, Afzal J, Rana MS, Imran M, Zhao X, et al. Modified Rice Straw Enhanced Cadmium (II) Immobilization in Soil and Promoted the

Degradation of Phenanthrene in Co-Contaminated Soil. Int J Mol Sci 2019;20.
[74] Rybicki BA, Nock NL, Savera AT, Tang D, Rundle A. Polycyclic aromatic hydrocarbon-DNA adduct formation in prostate carcinogenesis. Cancer letters 2006;239:157-67.
[75] E. M, P. T, X. Z, C. M, M.C. D. Strategic Role of Nanotechnology in Fertilizers: Potential and Limitations In: Rai M, Ribeiro C, Mattoso L, Duran N (eds) Emerging nanotechnologies in agriculture Springer, Cham 2015:25-68.
[76] Fujii M, Dang TC, Rose AL, Omura T, Waite TD. Effect of Light on Iron Uptake by the Freshwater Cyanobacterium Microcystis aeruginosa. Environmental Science & Technology 2011;45:1391.
[77] Kun Y, Lizhong Z, Baoshan X. Adsorption of polycyclic aromatic hydrocarbons by carbon nanomaterials. Environmental Science & Technology 2006;40:1855-61.
[78] del Rio LA, Lopez-Huertas E. ROS Generation in Peroxisomes and its Role in Cell Signaling. Plant and Cell Physiology 2016;57:1364-76.
[79] Song H, Wang Y-S, Sun C-C, Wang Y-T, Peng Y-L, Cheng H. Effects of pyrene on antioxidant systems and lipid peroxidation level in mangrove plants,Bruguiera gymnorrhiza. Ecotoxicology 2012;21:1625-32.
[80] Shen Y, Li J, Gu R, Yue L, Xing B. Carotenoid and superoxide dismutase are the most effective antioxidants participating in ROS scavenging in phenanthrene accumulated wheat leaf. Chemosphere 2018;197:513-25.
[81] Jia WL, Wang CP, Ma CX, Wang JC, Sun HW, Xing B. Mineral elements uptake and physiological response of Amaranthus mangostanus (L.) as affected by biochar. Ecotoxicol Environ Saf 2019;175:58-65.
[82] Maxwell K, Johnson GN. Chlorophyll fluorescence—a practical guide. Journal of Experimental Botany 2000;51:659-68.
[83] Baker NR. Chlorophyll fluorescence: a probe of photosynthesis in vivo. Annu Rev Plant Biol 2008;59:89-113.
[84] Kramer DM, Johnson G, Kiirats O, Edwards GE. New fluorescence parameters for the determination of QA redox state and excitation energy fluxes. Photosynthesis Research 2004;79:209-18.
[85] Kurisu G, Zhang H, Smith JL, Cramer WA. Structure of the cytochrome b6f complex of oxygenic photosynthesis: tuning the cavity. Science 2003;302:1009-14.
[86] Adamiec M, Misztal L, Kosicka E, Paluch-Lubawa E, Luciński R. Arabidopsis thaliana egy2 mutants display altered expression level of genes encoding crucial photosystem II proteins. Journal of plant physiology 2018;231:155-67.
[87] Rubio-Moraga A, Rambla JL, Fernández-de-Carmen A, Trapero-Mozos A, Ahrazem O, Orzáez D, et al. New target carotenoids for CCD4 enzymes are revealed with the characterization of a novel stress-induced carotenoid cleavage dioxygenase gene from Crocus sativus. Plant molecular biology 2014;86:555-69.
[88] Ryle MJ, Hausinger RP. Non-heme iron oxygenases. Current opinion in chemical biology 2002;6:193-201.
[89] Ohmiya A. Carotenoid cleavage dioxygenases and their apocarotenoid products in plants. Plant Biotechnology 2009;26:351-8.

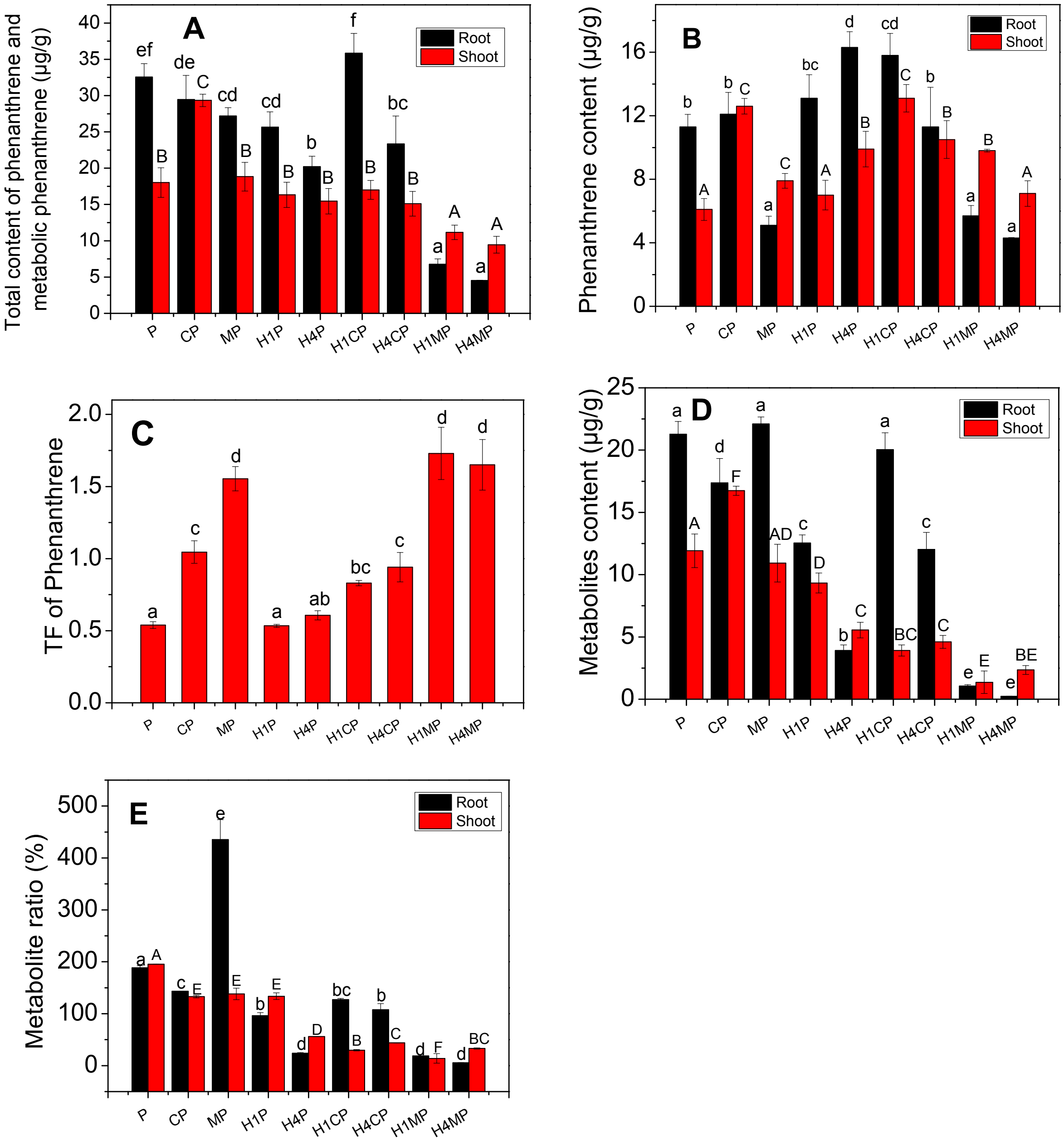

Figure 1. Phe and its metabolite content in lettuce treated with Phe (P), carbon nanotubes (C), magnetic carbon nanotubes (M), and different fractions of DHA (DHA1 and DHA4). Figure A, B, C, D and E represents total content of Phe and its metabolic Phe, total Phe content, translocation factor of Phe from root to shoot (TF of Phe), total Phe metabolites content, as well as the ratio between metabolites and Phe, respectively. Different letters in each panel represent that the data points are significantly different at $p < 0.05$ (Duncan's test).

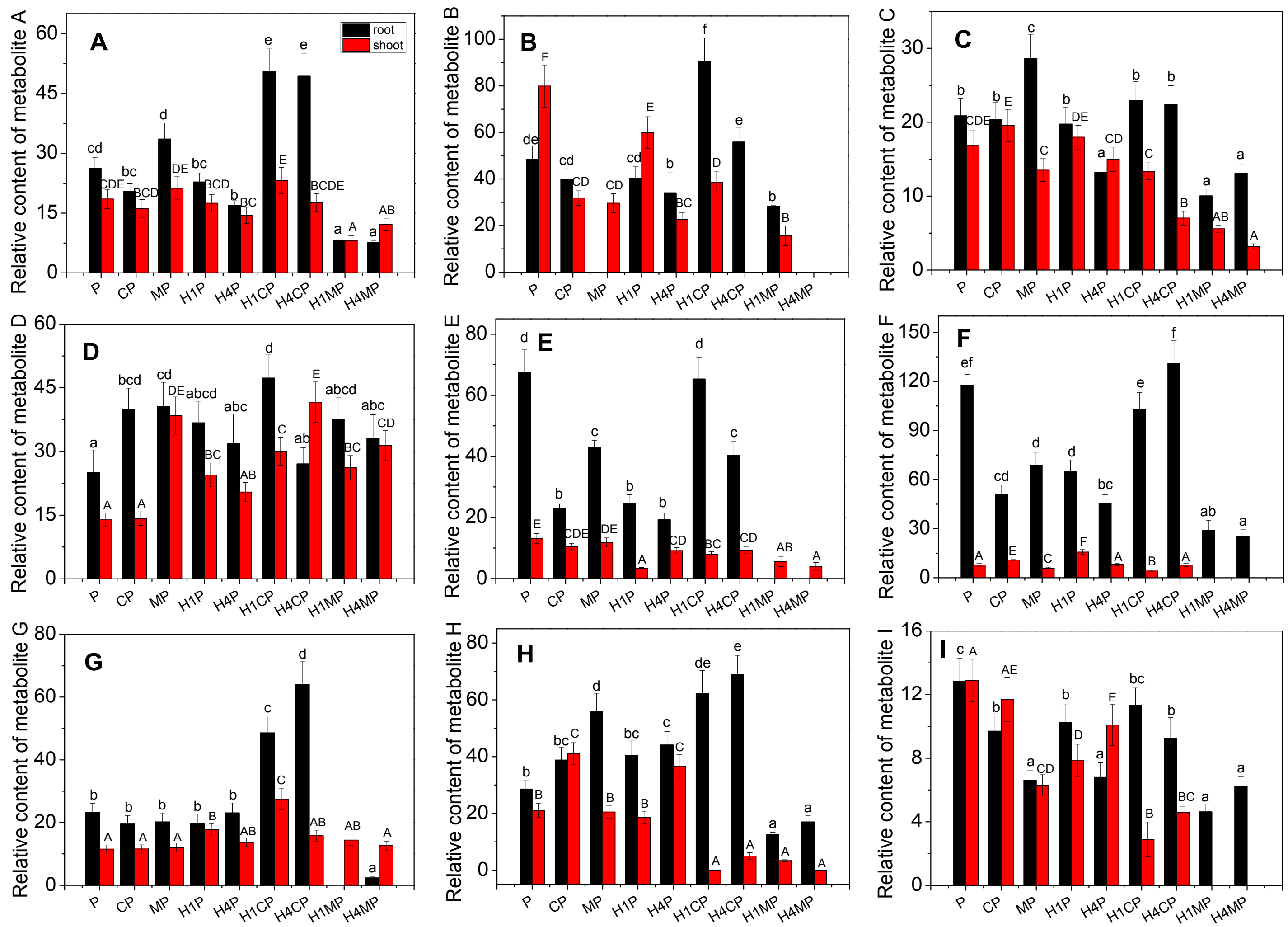

Figure 2. Relative content of different Phe metabolites in lettuce treated with Phe (P), carbon nanotubes (C), magnetic carbon nanotubes (M), and different fractions of DHA (H1 and H4). Figure A-I represent relative Phe metabolite content of *trans*-2,3-dioxo-5-(2'-hydroxyphenyl)-pent-4-enoic acid, phthalic acid, salicylic acid, protocatechuic acid, 2,4-dihyoxybenzoicacid, 2,3-dihyoxybenzoicacid, p-hydroxy benzoic acid, 3-hydroxybenzoic acid and benzoic acid, respectively. Different letters in each panel represent that the data points are significantly different at $p < 0.05$ (Duncan's test).

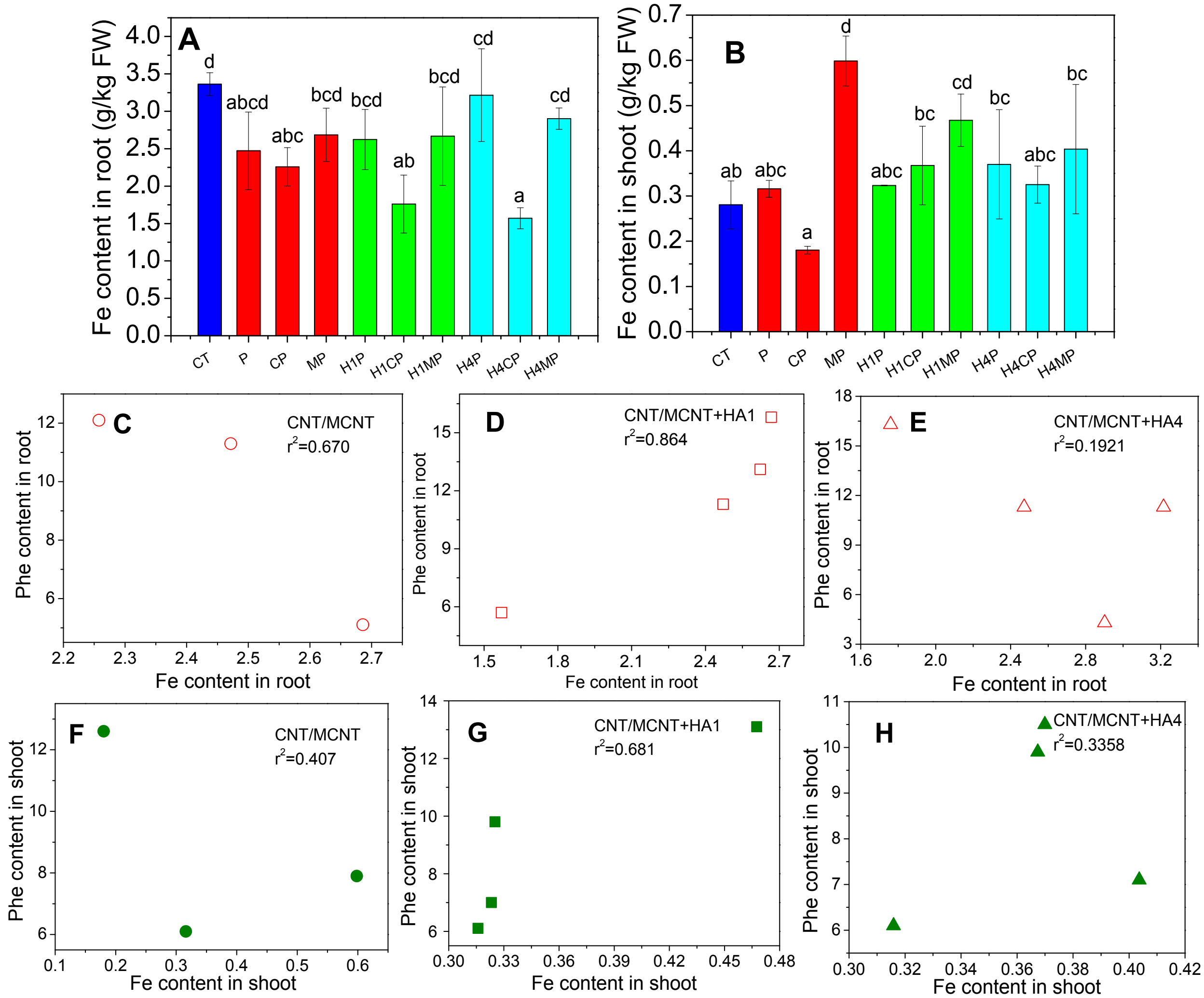

Figure 3. Fe content in lettuce and the correlation between the Fe and Phe content across all treatments (Note: Phe (P), carbon nanotubes (C), magnetic carbon nanotubes (M), and different fractions of DHA (H1 and H4)). Figure A and B represent Fe content in root and shoot, respectively. Figure C-E represents the correlation between Fe and Phe content in the treatment with carbon nanomaterials alone, carbon nanomaterials+DHA1, carbon nanomaterials+DHA4 in roots, respectively. Figure F-H represents the correlation between Fe and Phe content in the treatment with carbon nanomaterials alone, carbon nanomaterials+DHA1, carbon nanomaterials+DHA4 in shoots, respectively. Different letters in each panel represent that the data points are significantly different at $p < 0.05$ (Duncan's test).

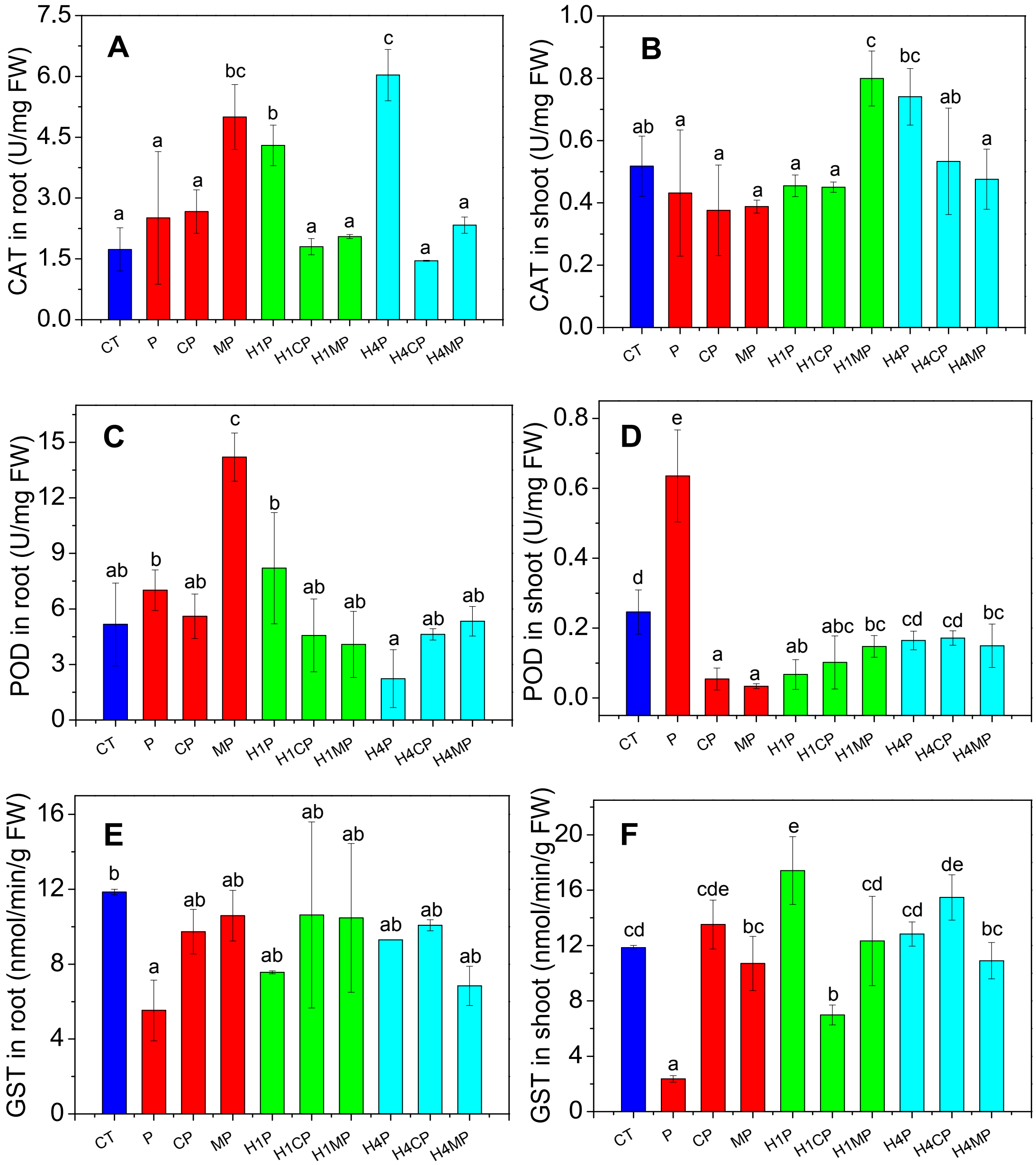

Figure 4. Antioxidant defense response of lettuce exposed to Phe under different treatments (Note: Phe (P), carbon nanotubes (C), magnetic carbon nanotubes (M), and different fractions of DHA (H1 and H4)). Figure A-F represents CAT, POD and GST enzyme activity in roots and shoots, respectively. Different letters in each panel represent that the data points are significantly different at $p < 0.05$ (Duncan's test).

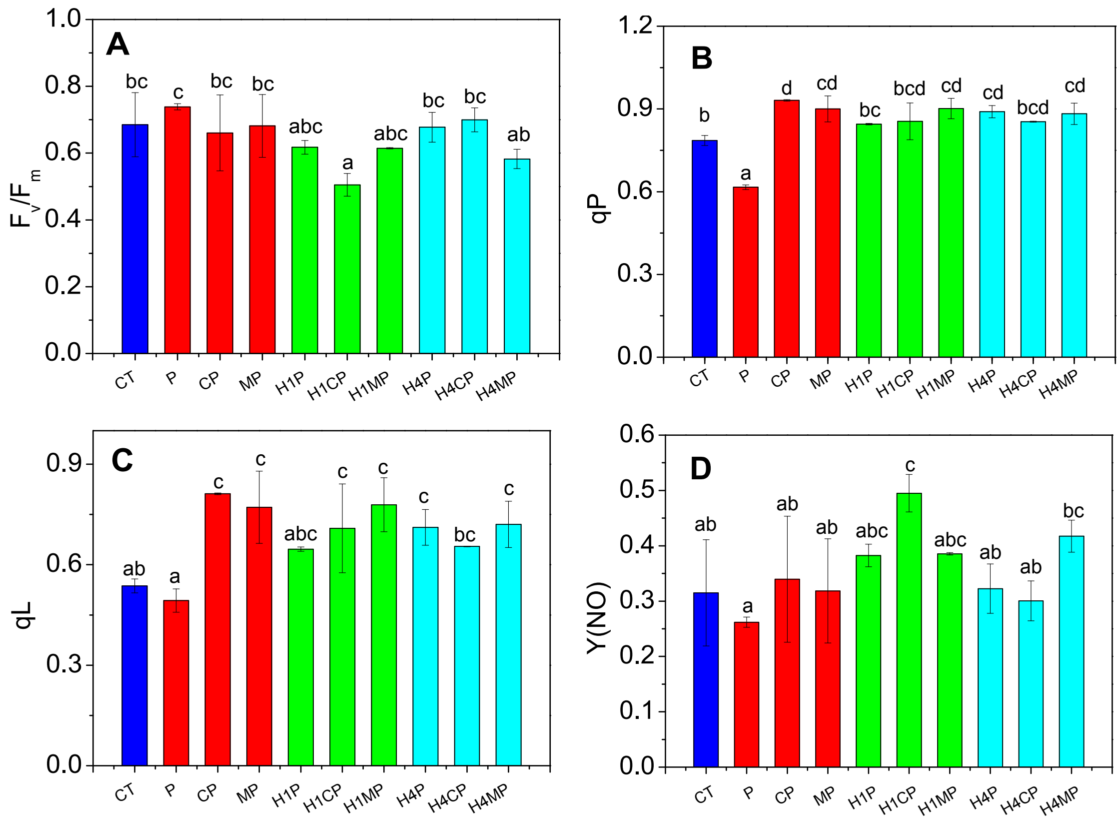

Figure 5. Photosynthetic system of lettuce exposed to Phe under different treatments (Note: Phe (P), carbon nanotubes (C), magnetic carbon nanotubes (M), and different fractions of DHA (H1 and H4)). Figure A-D represents F_v/F_m- maximum quantum efficiency of PSII, qP- intensity of photochemical quenching coefficient (Swamp model), qL- intensity of photochemical quenching coefficient (Lake model), Y(NO)- Non-regulatory energy dissipation coefficient, respectively. Different letters in each panel represent that the data points are significantly different at $p < 0.05$ (Duncan's test).

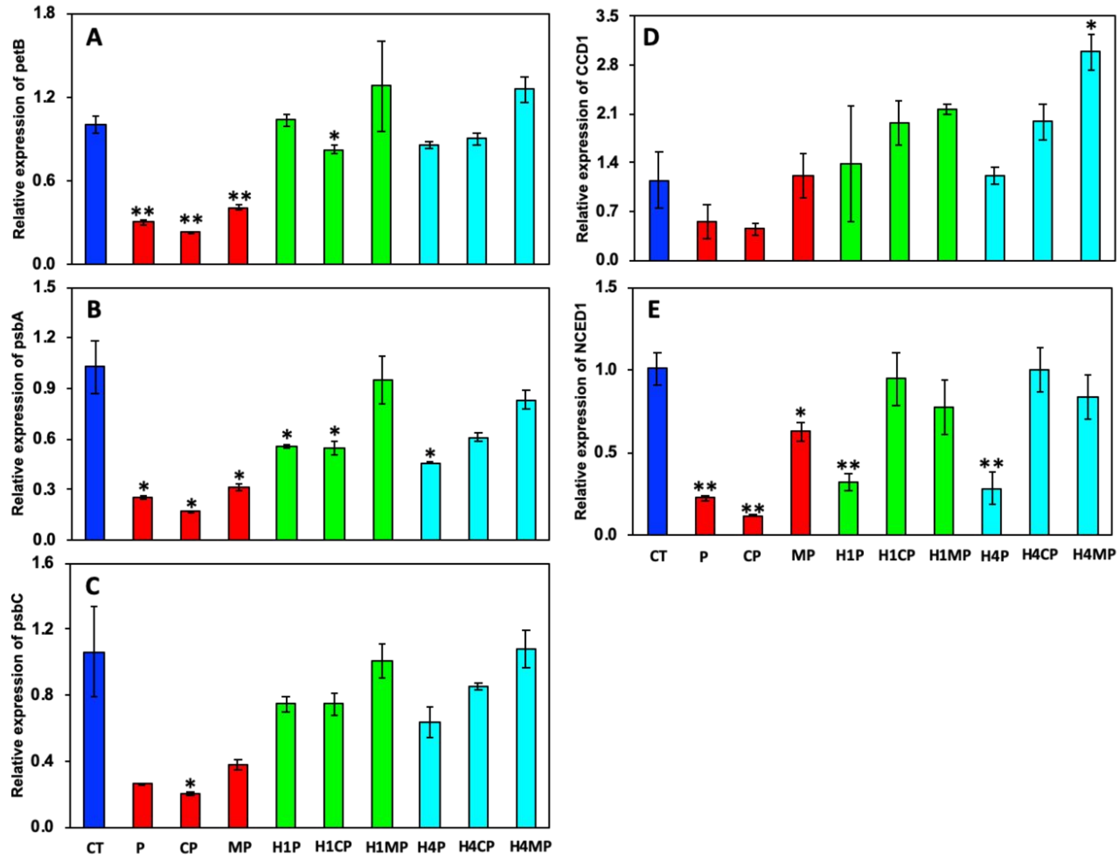

Figure 6. Relative expression of genes involved in photosynthesis II and secondary metabolite pathways in lettuce as affected by Phe, CNTs/MCNTs, and DHA1/DHA4 (Note: Phe (P), carbon nanotubes (C), magnetic carbon nanotubes (M), and different fractions of DHA (H1 and H4)). Figure A-C represents cytochrome b6 (petB), which mediates electron transfer between photosystem II (PSII) and photosystem I; photosystem II D1 protein (psbA), the primary electron donor of PSII; PSII CP43 reaction center protein (psbC), respectively. Figure D-E represents carotenoid cleavage dioxygenase 1 (CCD1), 9-cis-epoxycarotenoid dioxygenase 1 (NCED1), respectively. Single asterisk indicates the significant difference between control and each treatment at $p < 0.05$; double asterisks indicate the significant difference between control and each treatment at $p < 0.01$.

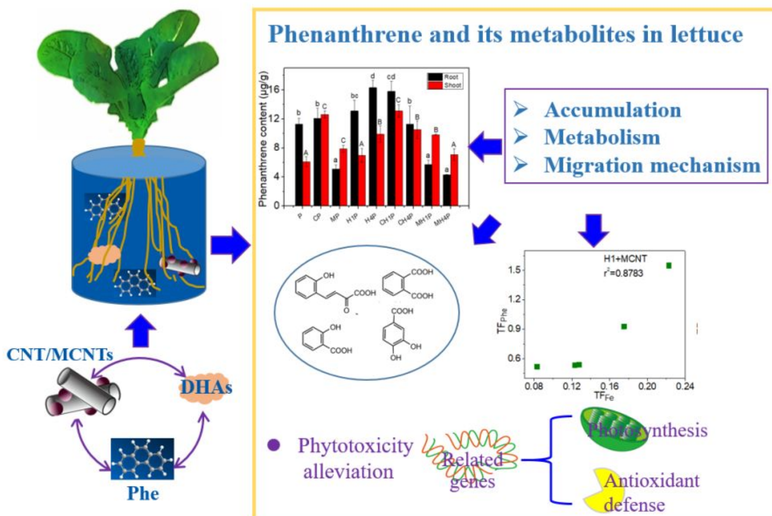
Phenanthrene and its metabolites in lettuce
Accumulation
Metabolism
Migration mechanism
CNT/MCNTs
DHAs
Phe
H1+MCNT
Phytotoxicity alleviation
Related genes
Photosynthesis
Antioxidant defense